Silibinin Feeding Alters the Metabolic Profile in TRAMP Prostatic Tumors: ^{1}H-NMRS–Based Metabolomics Study

Komal Raina,[1] Natalie J. Serkova,[2,3] and Rajesh Agarwal[1,3]

Departments of [1]Pharmaceutical Sciences and [2]Anesthesiology and Radiology, and [3]University of Colorado Cancer Center, University of Colorado Denver, Aurora, Colorado

Abstract

Herein, we evaluated for the first time silibinin efficacy on prostate cancer (PCa) metabolism in transgenic adenocarcinoma of the mouse prostate (TRAMP) model using quantitative high-resolution proton nuclear magnetic resonance spectroscopy metabolomics. Prostate tissues were from mice fed control or silibinin diet for 20 weeks. Comparative metabolic profiling indicated that antitumor effect of silibinin is accompanied by alteration in metabolic profile of TRAMP prostatic tumors as indicated by 6-fold (P = 0.016) increase in glucose content and 48% (P = 0.015) reduction in lactate levels. Increase in citrate use by prostate tissue also reversed with silibinin, as indicated by 3-fold (P = 0.01) increase in citrate levels in silibinin-fed group. Also, 61% and 50% (P < 0.01) decrease in cholesterol and phosphatidylcholine levels, respectively, was observed with silibinin. These results corroborate our earlier findings regarding PCa chemopreventive potential of silibinin in TRAMP model and warrant additional metabolic profiling in other silibinin-fed PCa tumor model tissues. This will help identify specific metabolic biomarkers altered during silibinin treatment, which when detected in clinical biopsies or noninvasive magnetic resonance spectroscopic studies could help monitor silibinin effectiveness against PCa malignancy. [Cancer Res 2009;69(9):3731–5]

Introduction

Recent studies have shown that metabolic profile of various cancerous/noncancerous tissues can be correlated with cell growth/death, specific tumor type, and pathologic stage of tumor (1–4). In this regard, metabolomics of prostatic tissues using magnetic resonance spectroscopy (in both *in vivo* and *in vitro* conditions) has helped to identify and establish the metabolic profiles specific to prostate cancer (PCa) malignancy (1, 5). Specific metabolic alterations, due to progression of tumor lesions in PCa patients, include a significant decrease of citrate (zinc metabolism), increased phosphocholine and phosphatidylcholine (PtdCho; phospholipid turnover), and increased glucose uptake in cancerous lesions (3, 5).

We recently reported PCa inhibitory effects of silibinin in various studies (6) and on PCa progression in transgenic adenocarcinoma of the mouse prostate (TRAMP) mice (7). The chemopreventive efficacy of silibinin on TRAMP prostate tumor growth, progression, invasion, migration, and metastasis was subsequently evaluated and established, together with analyses of the protein molecules possibly involved with silibinin efficacy (8). From a broader viewpoint, the limitation of this study was that silibinin efficacy was not discussed in terms of metabolic stabilization in prostate tumors. With the rationale that evaluation of anticancer efficacy of a drug is incomplete without determining its effect on metabolic profile of the tumor tissue, we carried out a metabolomics study on prostate tissues. We used quantitative high-resolution proton nuclear magnetic resonance spectroscopy (^{1}H-NMRS) to assess the metabolic profile of silibinin-treated TRAMP prostatic tissue to complement histopathologic and molecular data generated earlier (6–8). The working hypothesis was that, upon silibinin treatment, specific metabolic biomarkers will sensitively detect changes in prostate tissue. Such a study would, inarguably, not only provide us with a complete scenario of silibinin chemopreventive efficacy against PCa progression in TRAMP mice, but in terms of practical and translational aspects, further validate the clinical usefulness of this drug.

Materials and Methods

Prostate tissue. Archival (7) dorsolateral prostate tissue (n = 4) samples, stored at −80°C, of TRAMP/C57BL/6 mice fed control (n = 17) or 1% silibinin-supplemented diet starting age 4 wk for 20 wk (n = 16), were used to assess metabolic profile of tissues. All retrospective studies have been previously approved by our Institutional Animal Care and Use Committee.

Sample preparation. Prostate tissues were extracted using 8% perchloric acid as previously described (4, 9). Briefly, ~0.1 grams of frozen tissues were processed, and extracted hydrophilic metabolites were dissolved in 0.45 mL of deuterium oxide while lipids were dissolved in 0.6 mL of deuterated chloroform/methanol mixture (2:1, v/v) before ^{1}H-NMRS. All deuterated compounds were from Cambridge Isotope, Inc.

Quantitative ^{1}H-NMR analysis. ^{1}H-NMRS analyses were performed by NJS (blinded to the group assignment of samples) using a 500 MHz Bruker DRX system equipped with Bruker TopSpin software (Bruker Biospin, Inc.; ref. 9). An inverse TXI 5-mm probe was used for all experiments. To suppress water residue in extracts, a standard Bruker water presaturation sequence was used ("zgpr"). An external reference, trimethylsilyl propionic-2,2,3,3,-d4 acid (0.5 mmol/L for hydrophilic and 1.2 mmol/L for lipid extracts), was used for metabolite quantification of fully relaxed ^{1}H-NMR spectra and as a ^{1}H chemical shift reference (0 ppm). For metabolite identification, a two-dimensional -^{1}H, ^{13}C-HSQC (heteronuclear single quantum correlation) NMR sequence was used. The ^{1}H-NMR peaks for single metabolites were identified and referred to a metabolite chemical shift library. The absolute concentrations of single metabolites were then referred to the trimethylsilyl propionic-2,2,3,3,-d4 acid integral and calculated using one-dimensional WINNMR (Bruker Biospin, Inc.; ref. 9).

Results

From each prostate tissue, 38 individual water-soluble and lipid metabolites were quantified (Table 1). We also included 4 significant metabolite ratios into the Principle component analysis

Requests for reprints: Rajesh Agarwal, University of Colorado Denver, C238-P15, Research 2, 12700 East 19th Avenue, Room 3121, Aurora, CO 80045. Phone: 303-724-4055; Fax: 303-724-7266; E-mail: Rajesh.Agarwal@UCDenver.edu.

doi:10.1158/0008-5472.CAN-09-0096

Table 1. Quantitative metabolic profile of prostatic tumor tissues of 2 study groups: (*a*) control untreated TRAMP mice and (*b*) silibinin-treated TRAMP mice (1% w/w silibinin supplemented diet given for 20 wk)

	Metabolite	^{1}H-NMRS	δ, ppm	Untreated (μmol/gram)	Silibinin (μmol/gram)
1.	Aromatic amino acids	Hydrophilic	9.28-6.85	8.19 ± 3.77	12.71 ± 7.14
2.	Adenine	Hydrophilic	6.00	0.65 ± 0.75	0.24 ± 0.11
3.	Adenosine	Hydrophilic	5.87	0.47 ± 0.42	0.59 ± 0.49
4.	Glucose	Hydrophilic	5.23+4.64	0.45 ± 0.14	2.88 ± 1.39 $^{P < 0.01}$
5.	Nucleotides	Hydrophilic	4.43	0.93 ± 1.16	1.01 ± 0.94
6.	Myo-inositol	Hydrophilic	4.05	1.34 ± 0.65	2.34 ± 0.62 $^{P < 0.0001}$
7.	Creatine	Hydrophilic	3.93	2.04 ± 1.95	2.58 ± 0.63
8.	Polyols	Hydrophilic	3.82-3.58	10.04 ± 5.92	40.16 ± 18.05 $^{P < 0.03}$
9.	Glycine	Hydrophilic	3.56	2.53 ± 0.79	2.96 ± 1.23
10.	Taurine	Hydrophilic	3.43+3.26	9.38 ± 4.34	10.75 ± 0.70
11.	GPC	Hydrophilic	3.23	0.67 ± 0.34	1.43 ± 0.20 $^{P < 0.01}$
12.	PC	Hydrophilic	3.21	1.44 ± 1.24	2.19 ± 1.56
13.	Total choline	Hydrophilic	3.19	0.43 ± 0.29	1.70 ± 0.53 $^{P < 0.01}$
14.	Total creatine	Hydrophilic	3.03	2.64 ± 1.63	5.29 ± 1.30
15.	GSH	Hydrophilic	2.95	0.36 ± 0.55	0.67 ± 0.27
16.	Aspartate	Hydrophilic	2.82+2.63	0.33 ± 0.16	0.29 ± 0.05
17.	Citrate	Hydrophilic	2.66+2.53	0.61 ± 0.26	1.78 ± 0.30 $^{P < 0.01}$
18.	Total glutathione	Hydrophilic	2.48	0.59 ± 0.54	1.03 ± 0.59 $^{P < 0.04}$
19.	Glutamine	Hydrophilic	2.43	0.47 ± 0.29	0.47 ± 0.21
20.	Succinate	Hydrophilic	2.40	0.94 ± 0.20	0.98 ± 0.19
21.	Glutamate	Hydrophilic	2.35	2.54 ± 1.45	3.07 ± 0.26
22.	Total CH_2−, CH_3	Hydrophilic	2.25–1.95	4.37 ± 2.72	6.55 ± 0.89
23.	Acetate	Hydrophilic	1.91	0.79 ± 0.37	0.85 ± 0.54
24.	Arginine+lysine	Hydrophilic	1.73–1.67	0.80 ± 0.49	0.99 ± 0.10
25.	Alanine	Hydrophilic	1.47	2.33 ± 0.61	1.07 ± 0.34 $^{P < 0.03}$
26.	Lactate	Hydrophilic	1.32	11.16 ± 1.21	5.83 ± 2.11 $^{P < 0.01}$
27.	Hydroxybutyrate	Hydrophilic	1.19	0.29 ± 0.12	0.60 ± 0.29
28.	Essential amino acids	Hydrophilic	1.10–0.72	4.97 ± 2.87	5.88 ± 1.41
29.	MUFA	Lipids	5.42	20.48 ± 6.33	43.61 ± 29.05
30.	Triacylglycerol	Lipids	4.18	9.52 ± 2.72	21.47 ± 16.96
31.	Glycerol-lipids	Lipids	4.13–4.07	2.89 ± 2.11	5.89 ± 2.64
32.	PtdCho	Lipids	3.65	8.68 ± 2.61	4.36 ± 1.59 $^{P < 0.03}$
33.	Total cholines (lipids)	Lipids	3.22	13.31 ± 6.46	5.88 ± 2.78
34.	PtdEth	Lipids	3.19	1.94 ± 1.41	1.24 ± 0.73
35.	PUFA	Lipids	2.82	60.02 ± 9.13	48.68 ± 14.51
36.	Total fatty acids	Lipids	2.28	78.57 ± 17.55	114.74 ± 60.50
37.	Total lipids	Lipids	0.89	142.29 ± 30.92	163.93 ± 73.52
38.	Cholesterol	Lipids	0.68	13.07 ± 1.48	5.09 ± 2.00 $^{P < 0.004}$
39.	[Lactate/glucose]	Hydrophilic	N/a	26.68 ± 8.20	2.66 ± 1.93 $^{P < 0.005}$
40.	[PC/GPC]	Hydrophilic	N/a	2.05 ± 0.68	0.89 ± 0.30 $^{P < 0.04}$
41.	[PUFA/MUFA]	Lipids	N/a	3.09 ± 0.88	1.66 ± 0.74 $^{P < 0.05}$
42.	[$Cho_{lipids}/Cho_{hydrophilic}$]	N/a	N/a	67.57 ± 78.33	4.05 ± 3.19 $^{P < 0.0001}$

NOTE: All data are given in μmol per gram prostate tissue and presented as mean ± SD (n = 4 for each group). Absolute individual concentrations of distinguished biomarkers were analyzed by ANOVA followed by Tukey's *post hoc* test to identify the groups that differed significantly. The significance level was set at a P value of <0.05 for all tests (Sigma Plot-version 9.01, Systat Software and SPSS version 14.0; SPSS, Inc). Only selected ^{1}H-chemical shifts are reported for individual metabolites (which were used for metabolite quantification). Cho [l/ws], ratio of cholines in lipid and water-soluble fractions. Abbreviations: Cho, choline; GSH, reduced glutathione; MUFA, monounsaturated fatty acids; PC, phosphocholine; ppm, part per million (units for NMR chemical shifts); PtdEth, phosphatidylethanolamine; PUFA, poly-unsaturated fatty acids.

(PCA), such that, for each tissue, a total set of 42 variables was included into the multivariate data analysis. The PCA analysis allowed for precise group separation between untreated and silibinin-fed TRAMP mice (Fig. 1*A*). In the next step, individual metabolites were distinguished, which were responsible for group clustering in Fig. 1*A*. Total of 14 biomarkers contributed to group separation (Fig. 1*B*) and were related to citrate, glucose, phospholipid, osmolyte, and antioxidant metabolism (Fig. 2). The major contributors for group separations were increased concentrations for citrate, intracellular glucose, choline in the water-soluble fraction, glycerophosphocholine (GPC), and myo-inositol, as well as decreased values of lactate, cholesterol, and three ratios from glucose and phospholipid metabolism. To lesser extent, decreased alanine and PtdCho, but increased polyols, glutathione,

and the ratio of unsaturated fatty acids contributed to the group clustering.

One of the most important findings in this study is the preserved citrate concentration in prostate upon silibinin treatment, as indicated by ~3-fold ($P < 0.01$) increase in citrate levels in silibinin group (Fig. 2*A*). That the citrate generated for normal secretion functions of the prostate and zinc metabolism was not further used for cholesterol synthesis was indicated by 61% decrease ($P < 0.04$) in cholesterol levels in silibinin-fed group, indicating decreased cholesterogenesis (Fig. 2*C*).

Furthermore, a significant decrease in glucose use was seen in silibinin-fed animals. Increased glucose uptake, due to high energy requirement and high aerobic glycolytic activity—one of the major hallmarks of tumor metabolism—usually results in decreased intracellular glucose concentrations and high levels of lactate (10, 11). In our study, a significant increase in intracellular glucose ($P < 0.01$) with simultaneous decrease in lactate ($P < 0.01$) and alanine ($P < 0.03$; end-products of glycolysis) were seen after silibinin-feeding (Fig. 2*A*). Thus, the glycolytic coefficient (ratio of intracellular lactate to intracellular glucose) was decreased from 26.68 in controls to 2.66 in silibinin-fed animals ($P < 0.05$; Table 1; Fig. 2*A*).

Another significant metabolic pathway for tumor development is increased phospholipid turnover in cancer cells, due to their high proliferation rates (12). In a variety of tumors, PtdCho, the major phospholipid in cell membrane, is increased (13, 14). Silibinin not only decreased PtdCho values in prostate ($P < 0.03$; Fig. 2*B*), but also significantly altered PtdCho synthesis and catabolism, thus providing an evidence for targeted cell growth inhibition. The ratio of phosphocholine (phosphocholine-PtdCho precursor) to GPC (GPC-PtdCho catabolism) was significantly decreased after silibinin treatment ($P < 0.04$), mostly due to an increase in GPC concentrations ($P < 0.01$). Moreover, a significant inhibition of PtdCho synthesis can be seen in accumulation of cytosolic

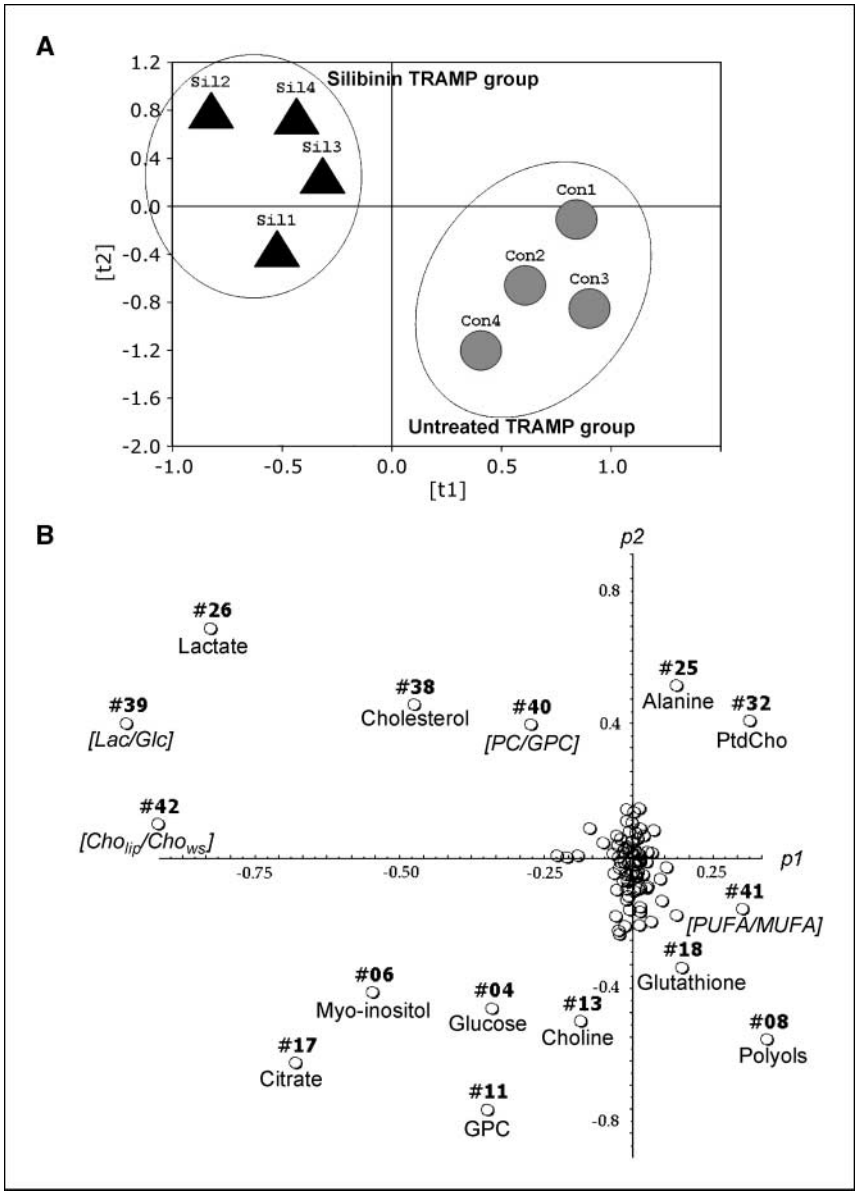

Figure 1. PCA on quantitative data sets for water-soluble and lipid metabolites, calculated from ^{1}H-NMR spectra of prostate tissue extracts. *A,* PCA scores (t_i) based on global metabolic pattern showed group separations between control and silibinin-treated TRAMP mice. *B,* PCA plots (p_i) on absolute concentrations of individual metabolites distinguish single putative biomarkers responsible for clustering pattern observed in *A*. Each circle represents an individual metabolite, which is assigned as a number of metabolite, according to Table 1. Briefly, PCA was applied to quantitative sets, which consisted of absolute individual concentrations of all metabolites obtained from two ^{1}H-NMRS data sets for each sample (^{1}H-NMR on water-soluble and lipid fractions). PCA prediction/classification (group clustering or "pattern recognition" visualization) and all mathematical models were built with AMIX software (3.5.1.; Bruker Biospin, Inc) followed by R package (2.00) on absolute concentrations of water-soluble and lipophilic metabolites.

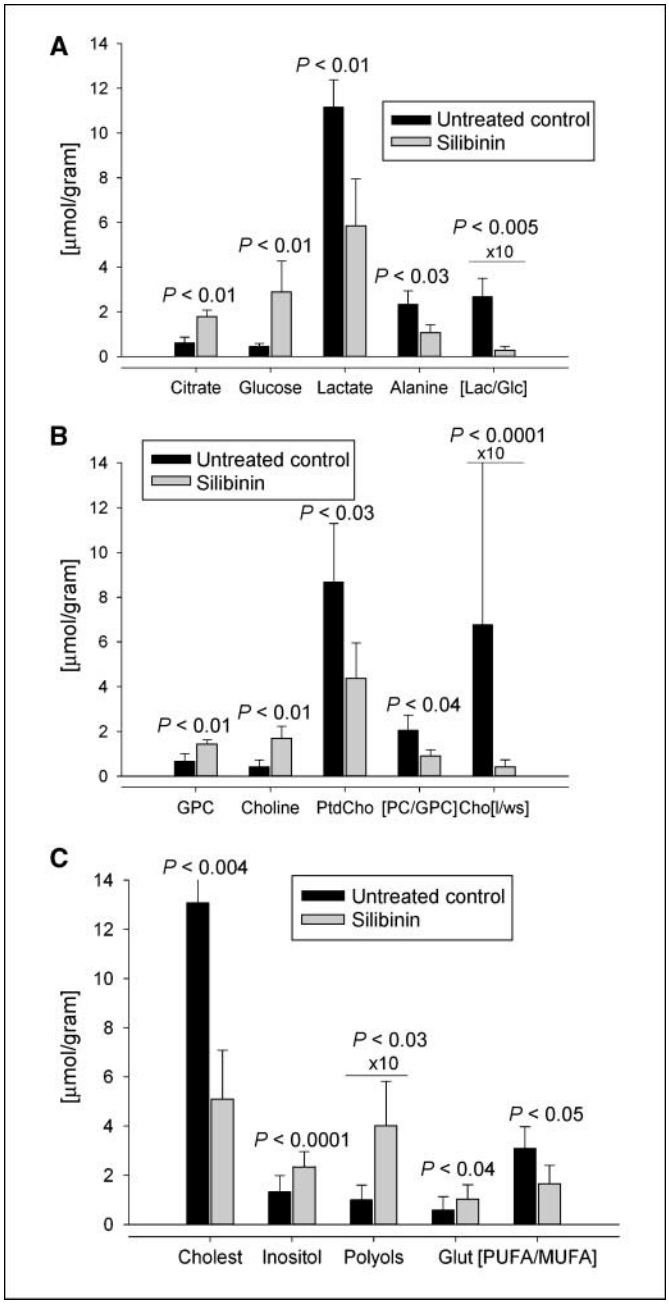

Figure 2. Validation of metabolites that were distinguished as biomarkers for metabolic changes after silibinin treatment (see Fig. 1*B*). *A* to *C*, plot individual concentrations [(μmol/g) prostate tissue, $n = 4$ for each data set] for each metabolite or metabolite ratios as calculated from ^{1}H-NMR spectra of hydrophilic and lipophilic fractions (Table 1).

hydrophilic choline ($P < 0.01$) and its dramatically decreased incorporation into membrane lipid fraction: the ratio of lipid-derived choline to cytosolic choline decreased from 67.6 to 4.1 in silibinin-fed animals ($P < 0.0001$; Table 1; Fig. 2*B*).

Increased concentrations of osmolyte myo-inositol ($P < 0.0001$) and other polyols ($P < 0.03$) were also observed in silibinin-fed group (Fig. 2*C*). Normal prostate glands express relatively high concentrations of polyols compared with PCa lesions. Higher levels of glutathione ($P < 0.04$) and decreased (poly-unsaturated fatty acids/monounsaturated fatty acids) ratios ($P < 0.05$) indicated improved antioxidant defense and decreased necrotic fraction under silibinin treatment.

Discussion

PCa progression in TRAMP mice mimics human PCa, developing spontaneous progressive stages of the prostatic disease with time (15–17). Earlier studies in TRAMP model indicate that silibinin reduces prostate adenocarcinoma incidence by slowing down tumor progression from prostatic intraepithelial neoplasia (premalignant) to adenocarcinoma (malignant) stages (7).

In the present study, metabolic profiling of TRAMP prostate tissues seemed to be highly sensitive to oral silibinin supplementation. Silibinin-related metabolic changes include the following: (*a*) normalization of citrate concentrations (for normal secretary functions of prostate), (*b*) decrease of glucose use and glycolytic activity, (*c*) decrease in membrane phospholipid synthesis, and (*d*) increase in polyols and antioxidants in prostate.

The results indicate that there is decreased glucose use by the prostatic tissue upon silibinin-feeding, which suggests decreased bioenergy requirements via fast glycolysis compared with untreated tumors that are highly proliferative and consume more glucose to meet their increased energy requirements. Thus, due to high activity of aerobic glycolysis in the untreated tumors, an increase in the end products of glycolysis (lactate and alanine) can be seen. There was also a significant reduction in lactate and alanine levels in silibinin-treated prostatic tissue, which resulted in decreased glycolytic coefficient.

Alteration in citrate levels upon PCa progression in TRAMP mice was found to mimic human PCa scenario, where a decrease in citrate levels is observed due to its increased use in Krebs cycle as well as to abnormal secretion functions and zinc metabolism. In normal human prostate, the glandular epithelial cells follow a metabolic pathway unlike other normal tissues (11, 18). In normal prostate epithelial cells (PEC), citrate is not a utilizable intermediate in Krebs cycle but an end product. This is likely due to accumulation of high levels of zinc in PEC of peripheral zone (the zone involved in PCa malignancy) than in other normal tissues (19). Zinc is involved in inhibition of m-aconitase (which converts citrate into iso-citrate in Krebs cycle), which results in an increase in net citrate production; the high amount of citrate is then secreted in the prostatic fluid. Thus, normal PEC unlike other normal mammalian cells are citrate-producing cells (18). Unlike other tumor types that end up being citrate producing, the malignant PEC have decreased levels of citrate as a consequence of decreased amounts of zinc (18). As a result, m-aconitase activity is not inhibited and citrate is used by the Krebs cycle. Although in normal PEC, 60% of energy derived from glucose is wasted due to citrate secretion, in malignant PEC, use of citrate in the Krebs cycle causes increased energy production and fatty acid synthesis to fulfill energy requirement of the fast proliferating PEC (18). These altered metabolic phenotype explains morphologic transformation from normal secretion cells to the fast proliferative tumor cells and is an essential metabolic adaptation to meet the increased bioenergetic demands of the neoplastic cells (11, 20). In the present study, one of the most significant observations was that silibinin was able to cause a reversal of citrate use in tumor cells and helped preserve the citrate concentration in prostatic tissue as it occurs in normal prostatic tissue, i.e., silibinin was able to restore the citrate producing characteristic and secretion functions of the

prostatic tissue. Furthermore, decrease in cholesterogenesis indicated that increased citrate was not being used for this process.

A variety of cancerous tissues including that of prostate exhibit altered metabolic profile of choline pathway intermediates (12, 13), specifically, the malignant tissues are characterized by elevated levels of PtdCho, the major membrane phospholipid, along with high levels of its precursor, phosphocholine (13, 14). Silibinin significantly decreased PtdCho levels and altered the PtdCho turnover in prostatic tissue as evidenced by increased GPC levels (PtdCho catabolic product) and a decrease in the content of lipid derived choline. The decreased ratio of phosphocholine/GPC by silibinin was also an interesting observation, as in some cancer cells, a switch from high GPC levels and low phosphocholine levels to low GPC and high levels of phosphocholine has been observed with increased malignancy (13). Whether this decrease in ratio by silibinin in TRAMP prostate can be interpreted as a positive inhibitory effect specific to TRAMP or is a general interference in choline phospholipid metabolism by silibinin, needs to be further investigated.

Silibinin feeding also significantly increased polyol levels that are significantly decreased during prostate tumor progression. There was also a significant increase in total glutathione levels in prostatic tissue by silibinin feeding compared with untreated controls, indicating that silibinin plays an inhibitory role in the progression of PCa by increasing the levels of the antioxidant glutathione, which serves as a free radical scavenger.

Whether the inhibitory effects of silibinin on PCa progression in TRAMP mice are via a direct interference in the metabolic pathway of various metabolites associated with malignancy in this PCa model or are a consequence of the normalizing effect that silibinin has on the malignant tissue via a genomic/proteomic response needs to be further investigated.

To the best of our knowledge, this is the first study of its kind, where the chemopreventive efficacy of an agent has also been evaluated in terms of the metabolomics of the tumors. The results corroborate our earlier findings and indicate the essential need to carry out such metabolic profiling in various other PCa tumor model tissues after treatment with a chemopreventive agent, including silibinin, so as to help identify the specific metabolites altered during the course of treatment, which when detected in clinical biopsies or noninvasive MRS studies can confirm the effectiveness of the agent against PCa malignancy.

Disclosure of Potential Conflicts of Interest

No potential conflicts of interest were disclosed.

Acknowledgments

Received 1/9/09; revised 3/5/09; accepted 3/6/09; published OnlineFirst 4/14/09.

Grant support: National Cancer Institute RO1 CA102514 and P30 CA046934. Metabolomics NMR Cancer Center Core facility was partly supported by Anesthesiology Department and National Cancer Institute P30 CA046934 Cancer Center Core Grant.

The costs of publication of this article were defrayed in part by the payment of page charges. This article must therefore be hereby marked *advertisement* in accordance with 18 U.S.C. Section 1734 solely to indicate this fact.

We thank Andrea Merz, B.S., for sample extraction.

References

1. Griffin JL, Kauppinen RA. Tumour metabolomics in animal models of human cancer. J Proteome Res 2007;6:498–505.
2. Griffin JL, Shockcor JP. Metabolic profiles of cancer cells. Nat Rev Cancer 2004;4:551–61.
3. Serkova NJ, Spratlin JL, Eckhardt SG. NMR-based metabolomics: translational application and treatment of cancer. Curr Opin Mol Ther 2007;9:572–85.
4. Serkova NJ, Niemann CU. Pattern recognition and biomarker validation using quantitative 1H-NMR-based metabolomics. Expert Rev Mol Diagn 2006;6:717–31.
5. Serkova NJ, Gamito EJ, Jones RH, et al. The metabolites citrate, myo-inositol, and spermine are potential age-independent markers of prostate cancer in human expressed prostatic secretions. Prostate 2008;68:620–8.
6. Singh RP, Agarwal R. Prostate cancer prevention by silibinin - bench to bedside. Mol Carcinog 2006;45:436–42.
7. Raina K, Blouin MJ, Singh RP, et al. Dietary feeding of silibinin inhibits prostate tumor growth and progression in transgenic adenocarcinoma of the mouse prostate model. Cancer Res 2007;67:11083–91.
8. Raina K, Rajamanickam S, Singh RP, et al. Stage-specific inhibitory effects and associated mechanisms of silibinin on tumor progression and metastasis in transgenic adenocarcinoma of the mouse prostate model. Cancer Res 2008;68:6822–30.
9. Serkova NJ, Rose JC, Epperson LE, Carey HV, Martin SL. Quantitative analysis of liver metabolites in three stages of the circannual hibernation cycle in 13-lined ground squirrels by NMR. Physiol Genomics 2007;31:15–24.
10. Baggetto LG. Deviant energetic metabolism of glycolytic cancer cells. Biochimie 1992;74:959–74.
11. Costello LC, Franklin RB. 'Why do tumour cells glycolyse?': from glycolysis through citrate to lipogenesis. Mol Cell Biochem 2005;280:1–8.
12. Ackerstaff E, Glunde K, Bhujwalla ZM. Choline phospholipid metabolism: a target in cancer cells? J Cell Biochem 2003;90:525–33.
13. Glunde K, Serkova NJ. Therapeutic targets and biomarkers identified in cancer choline phospholipid metabolism. Pharmacogenomics 2006;7:1109–23.
14. Glunde K, Jacobs MA, Bhujwalla ZM. Choline metabolism in cancer: implications for diagnosis and therapy. Expert Rev Mol Diagn 2006;6:821–9.
15. Gingrich JR, Barrios RJ, Foster BA, Greenberg NM. Pathologic progression of autochthonous prostate cancer in the TRAMP model. Prostate Cancer Prostatic Dis 1999;2:70–5.
16. Greenberg NM, DeMayo FJ, Sheppard PC, et al. The rat probasin gene promoter directs hormonally and developmentally regulated expression of a heterologous gene specifically to the prostate in transgenic mice. Mol Endocrinol 1994;8:230–9.
17. Gingrich JR, Greenberg NM. A transgenic mouse prostate cancer model. Toxicol Pathol 1996;24:502–4.
18. Costello LC, Franklin RB. The intermediary metabolism of the prostate: a key to understanding the pathogenesis and progression of prostate malignancy. Oncology 2000;59:269–82.
19. Costello LC, Franklin RB. The clinical relevance of the metabolism of prostate cancer; zinc and tumor suppression: connecting the dots. Mol Cancer 2006;5:17.
20. Costello LC, Franklin RB. Tumor cell metabolism: the marriage of molecular genetics and proteomics with cellular intermediary metabolism; proceed with caution! Mol Cancer 2006;5:59.